0273-2289/95/5601—0009$07.25

NMR Microscopy of Heavy Metal Absorption in Calcium Alginate Beads

NIKOLAUS NESTLE* AND RAINER KIMMICH

*Universität Ulm, Sektion Kernresonanzspektroskopie,
Albert-Einstein-Allee 7, D-89069 Ulm*

Received September 7, 1994; Accepted January 18, 1995

ABSTRACT

In recent years, heavy metal uptake by biopolymer gels, such as Cal-alginate or chitosan, has been studied by various methods. This is of interest because such materials might be an alternative to synthetical ion-exchange resins in the treatment of industrial waste waters. Most of the work done in this field consisted of studies of equilibirum absorption of different heavy metal ions with dependence on various experimental parameters. In some publications, the kinetics of absorption were studied, too. However, no experiments on the spatial distribution of heavy metals during the absorption process are known to us. Using Cu as an example, it is demonstrated in this article that NMR microscopy is an appropriate tool for such studies. By the method presented here, it is possible to monitor the spatial distribution of heavy metal ions with a time resolution of about 5 min and a spatial resolution of 100 μm or even better.

Index Entries: Heavy metal absorption; alginate; NMR microscopy; biopolymer gels, ion exchange.

INTRODUCTION

Alginate, made from certain brown seaweeds (e.g., *Fucus vesiculosus* or *Ascophyllum nodosum*) and also produced by some microorganisms (e.g., *Pseudomonas aeruginosa*) is an anionic polyelectrolyte consisting of blocks of mannuronic and guluronic acid. Depending on its origin, the ratio of guluronic and mannuronic acid varies, thus leading to different chemical and physical properties of the product.

---

*Author to whom all correspondence and reprint requests should be addressed.

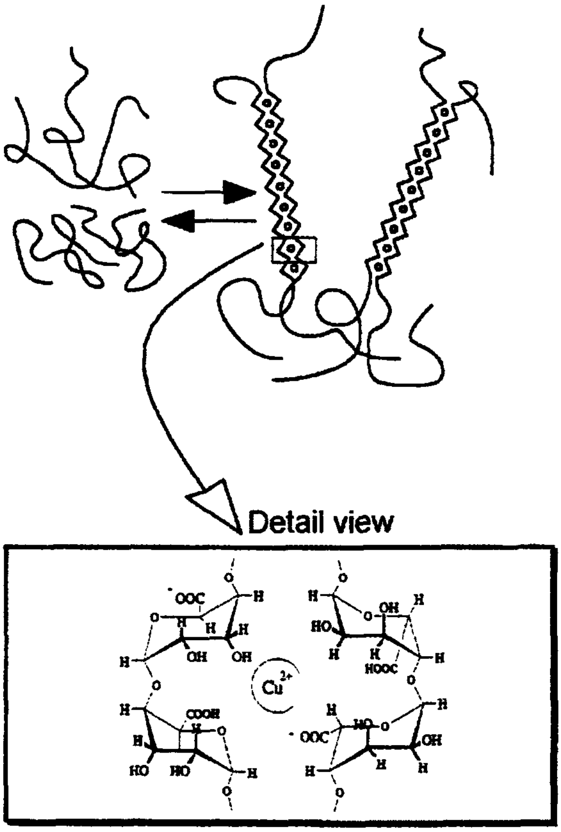

Fig. 1. Crosslinking of alginate by divalent ions (from *1*).

With monovalent positive counterions, alginates are soluble in water, leading to viscous sols. Brought in contact with most divalent ions, crosslinks develop between the guluronic segments of alginate chains, and a solid gel is formed. The crosslink structure responsible for gelling is depicted in Fig. 1.

Alginates are widely used in the food, textile, and pharmaceutical industries. In addition to this, alginates serve as an especially mild matrix for immobilizing cells and living tissues (e.g., 2). Another promising property of alginates is the ability to accumulate heavy metal ions from very dilute solutions (*3*). This phenomenon makes alginate as well as certain other biological polyelectrolytes, such as chitosan, interesting materials for the purification of industrial waste waters from such contaminations. Additionally, accumulation of heavy metals by the matrix might influence activity and metabolism of cells immobilized in alginate.

There have already been quite a few studies on heavy metal absorption either of pure calcium alginate or of pellets made from whole seaweeds (*4–6*). In these studies, it has been clearly demonstrated that such materials do have an interesting potential for technical application. In that work, absorption was mainly studied in equilibrium. In some studies, the kinetics of the absorption were monitored, too (*7,8*). In one more theoretical contribution, spatial aspects of heavy metal diffusion in the alginate beads were considered as well (*8*).

In this article, we introduce NMR microscopy (MRM) as an appropriate method for visualization of the spatial distribution of heavy metal ions in alginate gels. To our knowledge, up to now only pure calcium alginate has been studied by NMR imaging (*9*). From these experiments, it is known that water protons within a calcium alginate bead have an NMR relaxation time, T_2, of about 100 ms, which is considerably shorter than the one of free water, but still long enough to allow NMR-imaging studies. On absorption of many heavy metal ions, the relaxation time of alginate gels is reduced substantially to the order of a few milliseconds. This reduction is mainly the result of the paramagnetism exhibited by many heavy metal ions (e.g., Cr^{3+}, Cu^{2+}, Co^{2+}, Ni^{2+}, many ions of rare earth, and actinoid metals). In addition to paramagnetic effects, T_2 is affected by different types of chemical bonding with different heavy metal ions (length and stiffness of crosslinks, chelation effects).

As for NMR imaging of the absorption process, the reduction of T_2 offers a very good contrast in appropriate imaging sequences. By means of this contrast, it is possible to obtain a time-resolved series of NMR images visualizing the time dependence of the spatial distribution and absorption of heavy metal ions.

MATERIALS AND METHODS

Alginate

Sodium alginate samples (food grade) were obtained from Kelco, Hamburg, and Spinnrad, Gelsenkirchen. Because of their higher purity (higher transparency of the sol, no sea smell), the samples obtained from Spinnrad were used in most of our experiments. All other chemicals were of analytical grade and purchased either from Merck, Darmstadt, or from Fluka, Buchs SG.

Preparation of Alginate Beads

To produce C-alginate beads, the sodium alginate samples were dissolved in demineralized water at a concentration of 2% (w/v). This sol was pressed through a syringe with a 0.7-mm needle to drop into a beaker filled with 0.1*M* $CaCl_2$. The solution was stirred at about 50 rpm by means of a magnetic rotary shaker. The falling height of the drops was about 20 cm. This preparation resulted in the formation of approximately spherical beads of about 4-mm diameter. After formation, they were allowed to harden in the Ca chloride solution for several hours. The beads were then washed with tap water, put into demineralized water, and stored in a refrigerator at about 6°C until usage in the absorption experiments.

Setup for NMR Microscopy at 200 MHz

NMR microscopy was performed using a 40-cm bore Bruker Biospec 4.7 T superconducting magnet (Bruker, Rheinstetten, Germany) in combination with a homemade imaging electronic and a 4-cm bore gradient coil set and probe head obtained from Bruker. As a radio frequency coil, a homemade one turn saddle coil with an inner diameter of 13 mm was used.

The alginate beads were filled into a test tube made of a 3 mL LL disposable syringe (Becton Dickinson, Meylan, France) with an inner diameter of 8 mm. This type of test tube was selected because the heavy metal solution was circulated through the test tube in order to ensure a constant concentration throughout the experiments. Working with a constant ion concentration outside the beads reduces the number of time-dependent variables to the ion concentrations within the bead and, thus, simplifies quantitative considerations. The solution was circulated by a variable-speed pericyclic pump obtained from Roth Labortechnik (Karlsruhe). At the beginning of the experiments, the pump was used with maximum flow rate (about 110 mL/min) to remove all air from the flow circuit (before addition of heavy metal ions) and to assure good mixing of the solution (after addition of the ions). During the imaging experiment itself, the flow rate was reduced to about 4 mL/min in order to reduce the formation of flow artifacts. To maintain the concentration of the heavy metals as constant as possible, a reservoir of at least 2 L was provided within the flow circuit.

The NMR images were recorded using the standard gradient echo imaging sequence depicted in Fig. 2. The repetition time used in all experiments was 300 ms, and the echo time was 11 ms. The pixel size in all images was $(100\ \mu m)^2$ with a slice thickness of 1 mm.

Contrast in this imaging sequence is owing to T_2^*-relaxation, which is a result of both dephasing owing to magnetic field inhomogeneities as well as generic T_2-relaxation. As a result of good magnetic field homogeneity, we obtained a nearly pure relaxation contrast in our experiments.

Image Processing

Image data recorded in the experiments were processed using homemade software for baseline correction and Fourier transform. After Fourier transform, the images were converted into the Windows-BMP graphics format. This allows working with standard Windows programs for printing and for creating masks for background noise suppression and for further quantitative evaluations of the images. As appropriate software package for closer quantitative evaluation of the image series is presently being developed.

EXPERIMENTAL RESULTS AND DISCUSSION

Most of our experiments were run with Cu as a typical heavy metal ion. This is owing to several reasons:

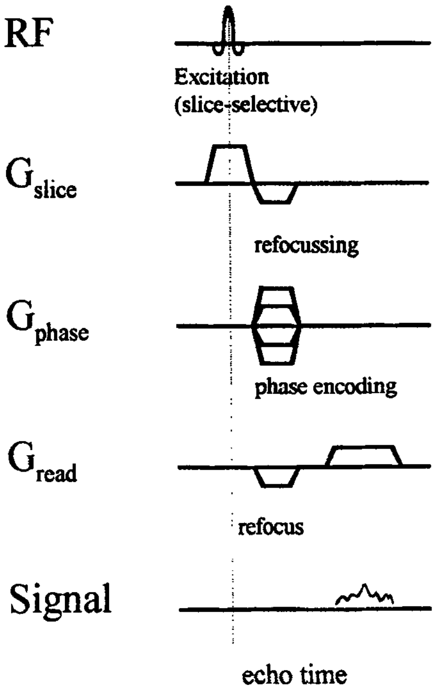

Fig. 2. Standard gradient echo sequence for NMR microscopy.

- In aqueous, nonliving NMR samples, Cu is a very common agent for reducing relaxation times T_1 and T_2;
- Cu exhibits an especially high affinity for alginate (*10*); and
- The absorption of Cu in alginate beads has recently been studied by several authors quite extensively (*8,11,12*).

In our experiments, we had $CuSO_4$ solutions of different concentrations circulate around a bed of Ca-alginate beads in a test tube. On exposing the beads to the copper solution, up to 120 subsequent NMR images were acquired in a time of about 10 h. From these pictures, the intrusion of heavy metal ions into the core of the beads can be seen very clearly (*see* Figs. 3–8).

As can be seen from the work presented here, NMR microscopy offers a good tool for time-resolved studies of the absorption of heavy metal ions into beads of Ca-alginate. A closer look at the images in Figs. 3–8 reveals several interesting phenomena: Throughout the absorption process, there is a sharp separation between dark and light regions in the beads. This implies that the copper-binding zone itself is relatively well defined, too.

The existence of the very sharp contrast between the solution and the beads also demonstrates the accumulation of Cu in the beads: Cu concentrations are many times higher there than in the circulating solution. The accumulation of Cu ions is obvious from the slow movement of the intrusion zone, too: A diffusion-limited ion uptake process would lead to an

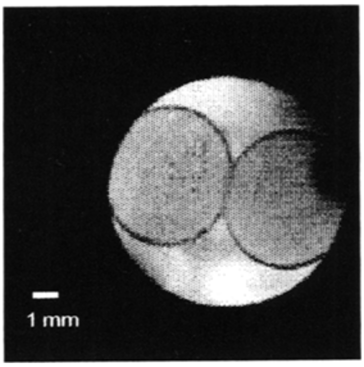

Fig. 3. Cross-section of a test tube containing two Ca-alginate beads about 10 min after adding 1 m*M* $CuSO_4$. The dark shade in the upper right edge of the right bead is caused by an internal air bubble in the bead.

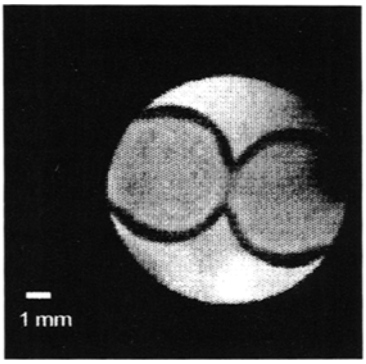

Fig. 4. Same structure, 1 h after addition of Cu.

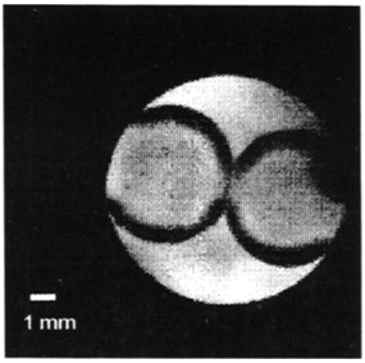

Fig. 5. Same structure, 2 h after addition of Cu.

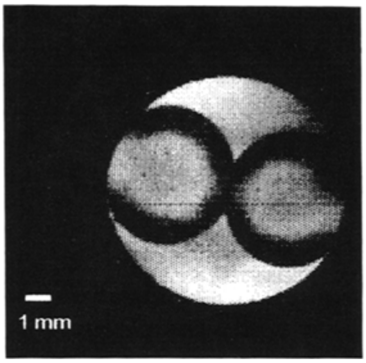

Fig. 6. Same structure, 4 h after addition of Cu.

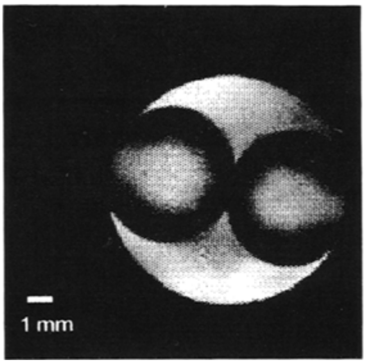

Fig. 7. Same structure, 7 h after addition of Cu.

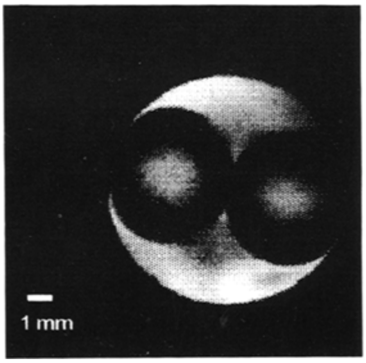

Fig. 8. Same structure, 10 h after addition of Cu.

intrusion depth of about 5 mm after 10 h when a diffusion coefficient for Cu ions of $3 \cdot 10^{-10} m^2/s$ in the alginate gel is assumed. This is a conservative estimate: Values between this and $1.84 \cdot 10^{-9} m^2/s$ are reported in the literature (*see 6,12*). However, our NMR images indicate a Cu ion intrusion of only about 2 mm in 10 h. This is in accordance with the results of Chen et al. (*8*) interpreted according to the Shrinking Core Model (SCM) (*13*). Thus, our results suggest that neither the SCM nor the linear absorption model (*14*), which was found to be superior to the SCM by Chen (*8*) gives a fully realistic description of the ion absorption process in alginates. We are presently working out a new theory in order to provide a better understanding of our results with respect to the earlier ones mentioned here.

Preliminary measurements performed with other heavy metal ions (Co, Ni) whose affinity to alginate is smaller than that of Cu show a different behavior of heavy metal intrusion with a more diffuse zone of absorption, which is much larger than in the case of copper. This is mainly owing to the fact that pure diffusion effects play a more important role with these ions.

Furthermore, the intensity of fluid exchange at the surface of the beads can be seen from the NMR images: Cu intrusion is deeper in regions with good circulation, whereas it is not as deep at the walls of the test tube. This observation leads to the question of whether Cu absorption is governed by the flow rate in our circuit or rather by the Cu concentration of the solution.

To test which influence on the absorption is stronger, we compared image series obtained with different concentrations of Cu. From these comparisons, we can definitely say that Cu concentration is the main factor determining the absorption speed, although local flow impediments clearly influence the form of the absorption zone (*see* Figs. 9 and 10). These flow effects are much more pronounced with small Cu concentrations (below 1 m*M*).

CONCLUSIONS AND FURTHER RESEARCH

Our results clearly demonstrate the potential of NMR microscopy in studying heavy metal uptake of alginate beads and other ion-exchanging gels. As demonstrated in this article, our method is limited to paramagnetic ions. An extention to other ion species is currently under investigation. For the experiment, already a few beads of the respective material are sufficient.

In order to compare our imaging results to theoretical models of heavy metal uptake, further imaging series and a quantitative calibration of the image contrast are presently performed. The latter task might turn out to be quite difficult, because a nonlinear relationship between heavy metal concentration and relaxation rates is to be expected.

REFERENCES

1. Rees, D. A. and Welsh, E. J. (1977), *Angewandte Chemie* **89,** 228–239.
2. Brodelius, P., Deus, B., Mosbach, K., and Zenk, H. (1979), *FEBS Lett.* **103,** 93–97.

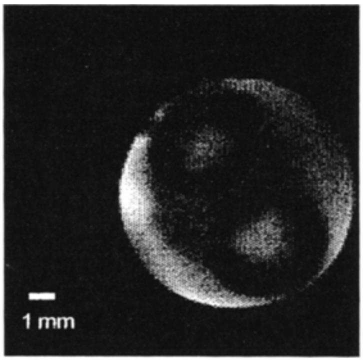

Fig. 9. Cross-section of two Ca-alginate beads 4 h after exposition to 2 m*M* $CuSO_4$ (the dark areas around the beads are probably the result of beads outside the image plane).

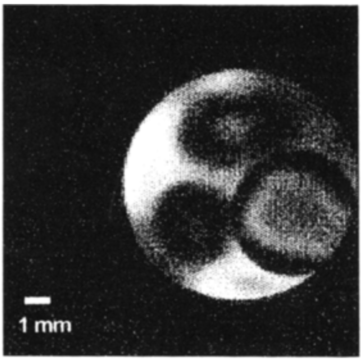

Fig. 10. Cross-section of a Ca-alginate bead 4 h after exposition to 0.5 m*M* $CuSO_4$ (the dark shades are two other beads not aequatorially cut by the image plane). Heavy metal accumulation is fastest where flow is not impeded by walls and other beads.

3. Ferguson, J. and Bubela, B. (1974), *Chem. Geol.* **13,** 163.
4. Kuyucak, N. and Volesky, B. (1989), *Biotechnol. Bioeng.* **33,** 823–831.
5. Holan, Z. R., Volesky, B., and Prasetyo, I. (1993), *Biotechnol. Bioeng.* **41,** 819–825.
6. Jang, L. K., Lopez, S. L., Eastman, S. L., and Pryfogle, P. (1991), *Biotechnol. Bioeng.* **37,** 266–273.
7. Kuyucak, N. and Volesky, B. (1989), *Biotechnol. Bioeng.* **33,** 809–814.
8. Chen, D., Lewandowski, Z., Roe, F., and Surapaneni, P. (1993), *Biotechnol. Bioeng.* **41,** 755–760.
9. Potter, K., Carpenter, T. A., and Hall, L. D. (1993), *Carbohydr. Res.* **246,** 43–49.
10. Haug, A. and Smidsrød, O. (1970), *Acta Chem. Scand.* **24,** 843–854.
11. Jang, L. K. (1994), *Biotechnol. Bioeng.* **44,** 183–185.
12. Lewandowski, Z. and Roe, F. (1994), *Biotechnol. Bioeng.* **44,** 186,187.
13. Rao, M. G. and Gupta, A. K. (1982), *Chem. Eng. J.* **24,** 181–190.
14. Crank, J. (1975), *Mathematics of Diffusion,* 2nd ed., Clarendon, London.